REACTIVE POWER FLOW OPTIMIZATION IN POWER SYSTEMS WITH HIERARCHICAL VOLTAGE CONTROL

Valentin Ilea[a], Cristian Bovo[a], Marco Merlo[a], Alberto Berizzi[a], Paolo Marannino[b†]
[a] Politecnico di Milano, Department of Energy, Via La Masa, 34 – 20156, Milano, Italy
[b] Universita degli Studi di Pavia, Strada Nuova, 65 – 27100,Pavia, Italy

Abstract – The Hierarchical Voltage Control (HVC) has been adopted in some countries as a significant improvement of the traditional voltage control solutions. This paper deals with the Optimal Reactive Power Flow (ORPF) from a Multi-objective perspective. In particular, it studies the interactions between three objective functions (OFs): one is the "traditional" real losses minimization, while the other two are designed to deal more directly with the electric network security. The three OFs have been integrated in a Multi-objective problem, adopting a new formulation of the Power Flow which includes a HVC model; a deep analysis on HVC complementarity constraints is presented. The new ORPF has been tested on a realistic model of the Italian Transmission System by using the high level modeling tool GAMS.

Keywords: optimal reactive power flow, hierarchical voltage control, security constrained OPF, complementarity constraints, multi-objective optimization

1 INTRODUCTION

In recent years, the control of voltages and reactive power has become more and more critical in the power system operation: the presence of the electricity market pushed the Transmission System Operators (TSOs) and the electrical utilities to exploit the transmission networks as close as possible to their security limits. To improve the voltage control in transmission grids, many projects have been developed around the world. Among these, the HVC is widely recognized as a viable solution and therefore it was adopted in some countries around the world [1] – [3].

Obtaining the set-points for the reactive resources by solving the ORPF problem is a key element in any voltage control scheme. Although the selection of adequate objective functions useful for the reactive power scheduling became to be under discussion since the time of the first modern control centers [4], the ORPF is usually treated so far as a minimum real losses problem. However, this approach takes roughly into account the network security. Under these circumstances, this paper analyzes the behavior of new objective functions, related directly with network security [5], in a Multi-objective approach [6]-[8], comparing their main characteristics with the ones of the real losses minimization. Moreover, particular interest is given to modeling, in a realistic manner, the behavior of the HVC using complementarity constraints. The approach gives the TSO a tool for the decision-making process. Once the Pareto set is determined, the Decision Maker, (DM, in this case, the TSO) has to choose the ultimate solution, that represents, from his point of view, the best compromise (when objectives are conflicting). Different methodologies are proposed in literature for selecting the Compromise Solution (CS) [9]-[11]. In any case, these methodologies require that the DM adopts appropriate criteria to select the CS. The solution depends on the criteria chosen by the TSO; therefore, in this paper, some considerations about possible criteria are discussed.

2 HVC STRUCTURE

Generally a HVC system is made by a primary level, given by the local action of the Automatic Voltage Regulators, a Secondary Voltage Control level (SVC) and a Tertiary Voltage Control level [1] (Fig. 1).

The SVC regulates a system area by controlling the voltage of the so-called pilot buses, representative for the voltage profile of the area load buses. Each pilot bus is regulated by the most effective area generators – the control generators – by changing their reactive output according to the area reactive level signal q. Thus, an equal reactive loading of all the control generators in each area is achieved. The adjustment of each generator is locally accomplished by acting on the set-points of the Automatic Voltage Regulators; this is performed, for each control area, by a secondary voltage regulator.

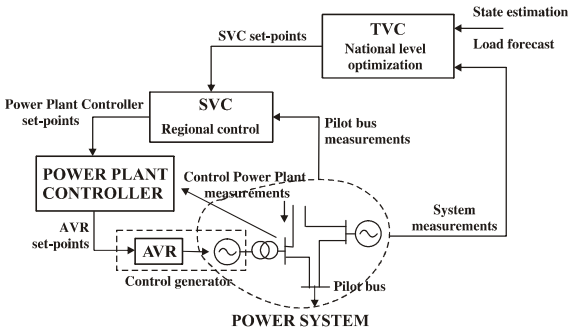

Figure 1: Structure of the hierarchical voltage – reactive power control system

The Tertiary Voltage Control provides a further closed control loop and coordinates the actions of the Secondary Voltage Regulators by computing the areas reactive levels set-points by means of a reactive power scheduling carried out on a very short term load forecast and on the on-line state estimator. The problem of coordinating the on-line reactive power scheduling given by an ORPF program and the three-level hierarchical voltage control of the transmission system network of the ENEL was deeply analyzed in [12].

3 BASIC ORPF MODEL

In the present section, the considered objective functions are presented. The approach adopted is specifically addressed to the reactive problem neglecting both eco-

nomical and (N-1) issues to highlight the features of the proposed model. However, the latter issues can be taken into account by including the relevant equations as optimization constraints.

3.1 Objective functions

Three OFs, relevant to different optimization strategies, were implemented [5][13]:

i) *minimizing the real power losses* in the branches of the considered network is currently used by TSOs worldwide to reduce the operating costs and, under the environmental issues, to reduce the CO_2 emissions. In this approach, the security is implicitly guaranteed by the respect of the operational limits [5]. To simplify the model, the losses minimization was obtained by minimizing the real power produced by the slack generator:

$$\min P_{SL} \tag{1}$$

where P_{SL} is the real power at the slack bus.

ii) *minimizing the reactive power output of the generators*, with the purpose of determining an optimal point in which the system has a sufficient regulation margin, granting to the power system a significant reserve of reactive resources against possible perturbations:

$$\min \sum Q_{g,i}^2 \tag{2}$$

where $Q_{g,i}$ is the reactive output of the i_{th} generator.

iii) *maximizing the loadability factor* (λ), seen as the distance of the current operating point from the point of collapse of the network (e.g., the critical point of the PV curves) [13][14]. This function is specially designed to optimize the security of the network:

$$\max \lambda \tag{3}$$

where λ is rate of load increase at every PQ bus, with respect to the initial value. Hence:

$$P_{Dj,\lambda} = P_{Dj,0} + \lambda P_{Dj,0} \tag{4}$$

where $P_{Dj,0}$ is the initial load and $P_{Dj,\lambda}$ is the load value for a given λ.

A corresponding increment in the reactive power demand is also assumed:

$$Q_{Dj,\lambda} = Q_{Dj,0} + \lambda P_{Dj,0} a \tag{5}$$

where a is a constant parameter depending on the chosen load-power factor. In this paper, a constant power factor equal to 0.9 in every bus is assumed:

$$a = \tan(\text{acos}(0.9)) \tag{6}$$

The load increases are satisfied by corresponding increments in the real power generations, computed as:

$$P_{Gi,\lambda} = P_{Gi,0} + \Delta P_{Gi}(\lambda) \tag{7}$$

where $\Delta P_{Gi}(\lambda)$ represents the increment of power generation at each generator. It is computed as a function of λ and according to the margins of each generator.

3.2 ORPF constraints

All the above OFs are subject to the same equality and inequality constraints. In this section a careful presentation is furnished.

The equality constraints consist of the power flow equations:

$$P_k - \boldsymbol{f}_{P_k}(\boldsymbol{V}, \boldsymbol{\theta}) = 0,\ k=1...N \tag{8,a}$$

$$Q_k - \boldsymbol{f}_{Q_k}(\boldsymbol{V}, \boldsymbol{\theta}) = 0,\ k=1...N \tag{8,b}$$

Then, for each area, it is necessary to add the SVC alignment conditions [12]:

$$\frac{Q_1}{Q_{1,\max}} = \ldots = \frac{Q_j}{Q_{j,\max}} = \ldots = \frac{Q_{n_c}}{Q_{n_c,\max}} = q,\ i=1...n_c \tag{9}$$

where:

P_k is the real power injection at bus k;

Q_k is the reactive power injection at bus k;

N is the number of buses in the system;

j is the index of the control generators in one area;

n_c is the number of control generators in one area;

q is the reactive level of one area;

and the subscript "max" denotes the upper capability limit.

The OFs are also subject to inequality constraints given by the bus voltage magnitudes limits and the capability limits of the generators:

$$V_{k,\min} \le V_k \le V_{k,\max} \tag{10.a}$$

$$Q_{Gi,\min} \le Q_{Gi} \le Q_{Gi,\max} \tag{10.b}$$

where:

$V_{k,\min/\max}$ are the lower/upper bounds of the bus voltage magnitudes, V_k;

$Q_{Gi,\min/\max}$ are the lower/upper bounds of the supplied reactive power, Q_{Gi}.

In what regards the generator models, the ones not participating in SVC will be modeled as conventional generators, i.e. represented as PV buses that shift to PQ when the reactive limits are reached. For the latter generators, the complementarity constraints model [13][15] is employed:

$$\begin{aligned} &\left(Q_{Gi} - Q_{Gi,\min}\right)\Delta V_i \le 0 \\ &\left(Q_{Gi} - Q_{Gi,\max}\right)\Delta V_i \le 0 \quad i \in \boldsymbol{PV} \\ &V_i = V_{i,0} + \Delta V_i \end{aligned} \tag{11}$$

where ΔV_i is the change in voltage of the i_{th} PV bus when one of the reactive limits is reached.

The control generators are represented as P-bus type [13][16] as their role is to keep the pilot bus voltage at the requested set-point thanks to the necessary reactive support. As consequence, in the power flow computation, the pilot buses are modeled as PVQ buses, i.e. PQ buses with imposed voltage. However, the purpose of this ORPF is to determine their optimal voltage profile and, hence, they will be represented as PQ buses.

While the above constraints apply to all OFs, additional constraints are required for the solution of the max λ problem. In particular, it is necessary to define two sets of constraints like (8)-(11). The first set holds for the initial equilibrium point of the system, where λ =0, and it is actually described by equations (8)-(11). The second set of equations is required to define the equilibrium point for $\lambda > 0$. In the latter case, the real and reactive powers are no longer constant but they are function of λ, according to (4), (5) and (7). The definition of the second set of constraints will also require doubling the set of variables:

$$P_{cr,k} - \boldsymbol{f}_{P_{cr,k}}(\boldsymbol{V}_{cr}, \boldsymbol{\theta}_{cr}) = 0 \qquad (12, a)$$

$$Q_{cr,k} - \boldsymbol{f}_{Q_{cr,k}}(\boldsymbol{V}_{cr}, \boldsymbol{\theta}_{cr}) = 0 \qquad (12, b)$$

where:

$P_{cr,k} = P_{Gk,\lambda} - P_{Dk,\lambda}$

$Q_{cr,k} = Q_{Gk,\lambda} - Q_{Dk,\lambda}$

and subscript *cr* represents the "doubled" set of variables.

In the same manner, equations (9)-(11), will be defined also for the *cr* variables. However, the minimum limits on the bus voltages are neglected as max λ requires the computation of the last point of convergence before voltage collapse, i.e. the mathematical critical point (MCP). Therefore, in this point, the voltage magnitudes could assume very low values.

A very important issue when maximizing λ, is the correlation between the power system security and the HVC scheme. A first simple approach is to assume that the pilot bus voltages in the initial and critical equilibrium points are kept equal:

$$V_{cr,r} = V_r \quad r \in \boldsymbol{PVQ} \qquad (13)$$

where ***PVQ*** is the set of pilot buses.

However, as the load increases, it is likely that the secondary control area reaches saturation, i.e. the control is lost (q_{crj} = 1); in this case, the optimization process would stop and λ cannot be further increased. In this situation, in order to compute a more realistic value of the loadability, the j_{th} pilot voltage is allowed to decrease when q_{crj}=1. In order to avoid structural changes in the model when the saturation of an area is reached, complementarity constraints are used, similarly to the PV bus constraints (11):

$$\begin{aligned} &\left(1 - q_{cr,r}\right)\Delta V_{cr,r} \le 0 \\ &V_{cr,r} = V_r - \Delta V_{cr,r} \quad r \in \boldsymbol{PVQ} \\ &\Delta V_{cr,r} \ge 0 \end{aligned} \qquad (14)$$

where $\Delta V_{cr,r}$ is the change in voltage of the j_{th} pilot bus when, in the critical operating condition, its area reaches saturation. Therefore:

i. when the HVC control is active, $q_{cr,r} < 1$ and $1 - q_{cr,r} < 0$, forcing $\Delta V_{cr,r}$ to be zero and, hence, (14) is equivalent to (13);

ii. when the control area is saturated $1 - q_{cr,r} = 0$, which allows $\Delta V_{cr,r}$ to take positive values and, hence, according to the second equation of (14) the voltage of the pilot bus in the critical point will decrease.

In what regards the impact of the HVC proposed models, i.e. equations (13) and (14), on the computation of λ the difference is depicted in Fig.2: if (13) is applied and a pilot bus reached its lower limit, the procedure stops at *MCP*_13; on the contrary, if (14) is adopted, *MCP*_14, the real critical point, could be reached. Technically, the *MCP*_13 is the maximum loadability that can be achieved with the HVC control active, while *MCP*_14 is the real indicator of system security. The differences between the two approaches are investigated in Section 4.

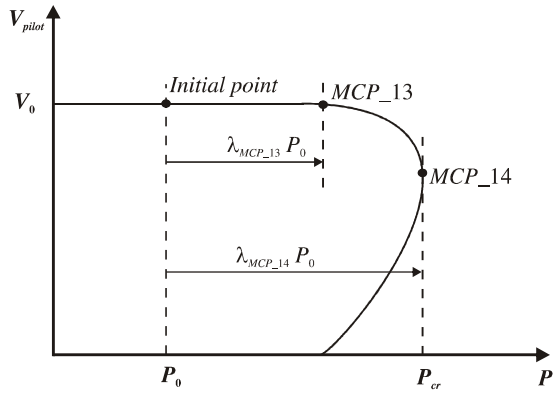

Figure 2: Representation of the computed critical point

3.3 Multi-objective approach

The Multi-objective can be applied when there are different conflicting OFs. In this case, there is not a unique solution of the problem, but any point belonging to the Pareto set could be chosen as a problem solution. This does not mean that all points are equivalent, but that each of them could be adopted as CS by the DM.

Therefore, the first step to solve a Multi-objective problem is to determine the Pareto set that can be computed through two equivalent methods: *the weights method* and *the* ε − *constraint method* [8]. The first one consists in defining a single objective function as a linear combination of the *N* considered objectives and let the optimizer solve the problem for a certain number of different weight combinations. The second one transforms *N*-1 objectives into constraints and optimizes the remaining function.

Preliminary tests showed a strong conflict between the three objectives, especially between max λ and the other two. Moreover, convergence problems were encountered adopting the *weight method*. To overcome this problem, the max λ OF is transformed into a constraint and a single objective function is defined as linear combination of the remaining two. In this way, a hybrid procedure between the two traditional methods was put in place:

$$\begin{aligned} &\min\left[\alpha P_{sl} + (1-\alpha)\sum Q_{g,i}^2\right] \\ &\text{subject to } \lambda \ge \mu \end{aligned} \qquad (15)$$

where:

α is the weight of P_{sl} in the Multi-objective function; it is increased by the solver from 0 to 1, in small steps;

μ is the minimum limit imposed on λ; after every α cycle the algorithm increases it in small steps in order to give more importance to max λ. Fig. 3 graphically depicts the procedure to compute the optimal-Pareto set.

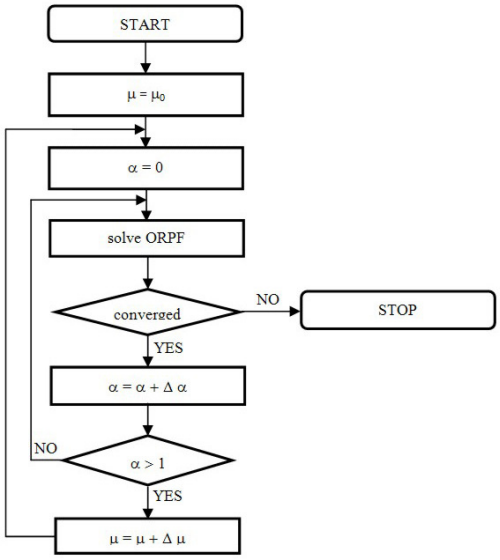

Figure 3: Flow-chart for the Pareto-set computation

3.4 Decision making approaches

To solve a Multi-objective problem, it is necessary to select a suitable CS from the Pareto-optimal set, process known as decision making [7]-[11]. This process can follow different approaches that can be divided in two classes: the methods of the first class find the CS automatically, once defined a single criterion of choice (for example, the minimization of the distance from the Utopia point that is the point whose co-ordinates in the objective space are given by the objectives optimized one at a time). The methodologies in the second class are based on interactive procedures, and the DM is stimulated to give his opinion on each alternative, in order to select the CS closest to his thinking. The disadvantage of these techniques is the need to calculate several points of the Pareto set and the greater complexity of the decision structure [11].

If the Utopia point criteria is adopted, in our case there are three objectives so, if we denote the ideal optimum by (x_0, y_0, z_0), the compromise solution (x_1, y_1, z_1) will be the one with:

$$D_1 = \min D_k \tag{16}$$

where:

$$D_k = \sqrt{(x_k - x_0)^2 + (y_k - y_0)^2 + (z_k - z_0)^2} \ .$$

However, each objective represents a different physical quantity and, hence, min D_k may not be a very reliable indicator, depending also on the adopted units. A solution could be the normalization of the OFs.

Another, more heuristic, approach is to start from a point of the Pareto-optimal set corresponding to the best value of one of the objectives and to move on the set in the direction of improving another objective until some desired compromise is reached. Then, the process can be continued in the direction of improving a third objective, and so on. In our case, from the TSO perspective, this process could be initiated from the point of minimum real losses. Then, as the security is an objective of particular importance, the move can be made in the direction of max λ, keeping the losses to the minimum as much as possible. Finally, when a desired compromise between P_{sl} and λ is reached, the move can be made in the direction of reactive production minimization, preserving the security. The final point of this process will be the CS.

4 TESTS AND RESULTS

The above mathematical model was implemented in GAMS [17], and solved using the COINIPOPT Solver 3.6. Two configurations of the Italian Transmission System were used for testing, named "Case A" and "Case B". The two networks are identically divided into 13 control areas - see [13] for details - but different loading conditions are simulated: the first one is characterized by a medium load, about 30100 MW ("Case A"), while the other is operating under more stressed conditions with a load level of about 34400 MW ("Case B"); this is the equivalent load as seen by the high voltage grid. The system consists of around 650 buses, 800 branches and 170 generators of which almost half are control generators: the model is complex and "realistic", useful to describe the response of the Italian transmission network.

4.1 Optimal Pareto-surfaces

Figure 4 depicts the comparison between the Pareto-sets for "Case A" obtained applying equations (13) or (14) to the HVC model, respectively. The Utopia points are represented with stars and their coordinates are given in Table 1. Moreover, for a clearer understanding, corresponding physical values are giving for each OF: the load margin for max λ, the total reactive production of the control generators for min $\Sigma\ Q^2$ and the real losses for min P_{sl}. To note that for λ the Utopia points are very close to the points obtained during the determination of the Pareto surface.

Looking at the results one can notice that, no matter the model adopted, all three objectives are in conflict: for a certain λ, the real losses increase as the reactive generation is minimized while both the real losses and reactive generation increase with λ. This is a general feature of this problem.

Comparing the two surfaces, it is possible to observe that the simplification (13) on PVQ busses brings high differences in all the cases where the weight on λ OF is high. In what regards the deviation introduced for the other two objectives, Figure 5 depicts the relative dif-

ferences computed as the normalized distance between two points, one on each surface, obtained in identical conditions (same μ and α), as long as there are corresponding points on each surface. Also in this case, the mismatch strongly increases with the weight on λ, reaching 120% for the maximum value of μ obtained by applying (13), i.e. μ = 0.28.

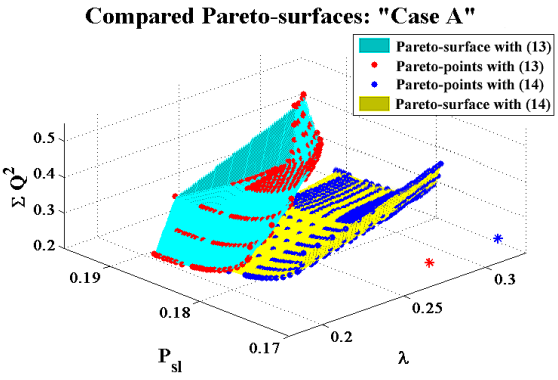

Figure 4: "Case A" Optimal Pareto-surfaces

λ_{MCP_14}	λ_{MCP_13}	ΣQ^2	P_{sl}
0.324	0.2823	0.213	0.173
Load Margin		$\Sigma\Sigma Q_k^r$	P_{loss}
9743 MW	8490 MW	3511 Mvar	291 MW

Table 1: Utopia points in "Case A". Objective functions and the corresponding physical values.

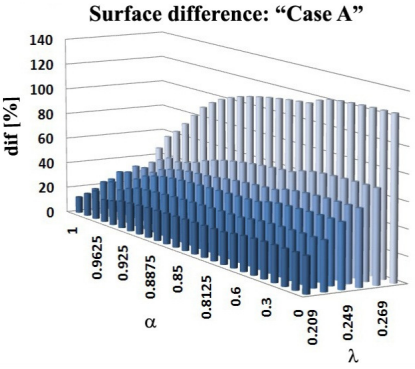

Figure 5: Relative difference introduced by (13) with respect to (14): "Case A"

The results obtained for "Case B" are reported in Figure 6 and Table 2, respectively. In this case, the surfaces are flatter than for "Case A": the cause is the reduced degree of freedom of the control variables caused by the higher loading level of the network, which also explains the increased values for min P_{sl} and $\min \sum Q_{g,i}^2$ and the smaller max λ.

Compared with "Case A", the differences between the proposed models, (13) and (14), are much higher: Δλ=0.09. This can be explained because the simplified model (13) gives higher differences with the increase of network stress, i.e. for conditions in which the reactive resources of the system are closer to the saturation.

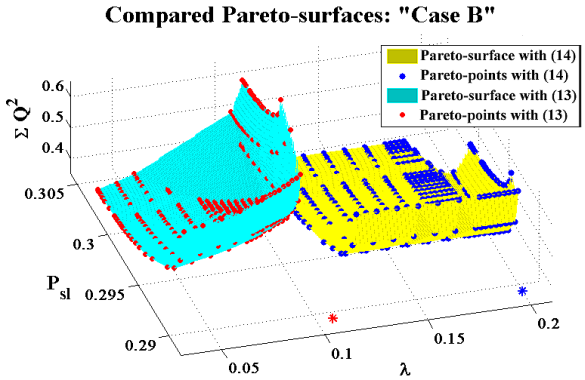

Figure 6: "Case B" Optimal Pareto-surfaces.

λ_{MCP_14}	λ_{MCP_13}	ΣQ^2	P_{sl}
0.202	0.11	0.328	0.29
Load Margin		$\Sigma\Sigma Q_k^r$	P_{loss}
6711 MW	3655 MW	4810 Mvar	383 MW

Table 2: Utopia points in "Case B". Objective functions and the corresponding physical values.

Looking at the above results it is clear that the simplified model (13) introduces unacceptable underestimation of the loadability. This makes the complementarity model based on (14) particularly suitable for power systems where electricity markets are likely to stress the system, even if computationally it is more challenging.

4.2 Decision making strategies

Taking into account the above conclusions, in this section only the results obtained using model (14), are reported. Figure 7 shows the Pareto-optimal surface obtained for "Case A". The application of the minimum distance from the Utopia point criterion, delivers us two points: p1 – if (16) is directly applied, and p2 – if D_k is computed using normalized OF values. Table 3 reports the coordinates of such points. The obtained voltage profiles are similar (see Figure 8), a little bit lower for p2 as the losses are higher. The results obtained from this first decision making approach are considered not satisfactory, motivating the application of the heuristic approach proposed in section 3.4.

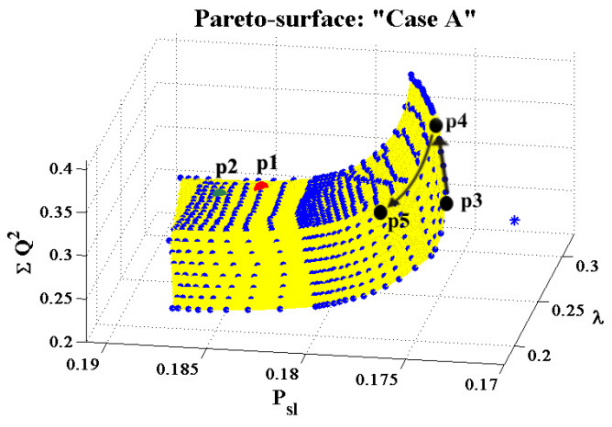

Figure 7: Decision making: "Case A"

	ΔP [MW]	$\sum\sum Q_k^r$ [Mvar]	λ	Load Margin [MW]
p1	303.8	3657	0.3115	9370
p2	305.8	3661	0.3065	9216
p3	291.7	4513	0.209	6450
p4	293.7	4643	0.27	8150
p5	296.6	4011	0.27	8150

Table 3: DM points: "Case A"

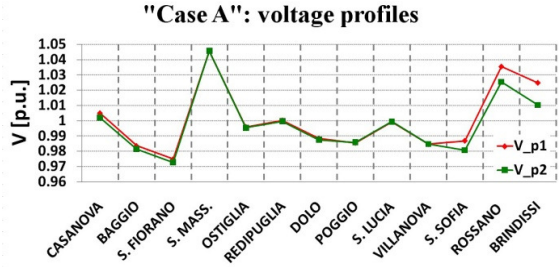

Figure 8: Voltage profiles: minimum distance DM criterion

The starting point chosen for the heuristic procedure corresponds to the classical minimization of the real losses (point p3 in Figure 7). Table 3 shows that, compared to p1 or p2, p3 has a lower loadability and the reactive production is very high. However, in Figure 9 we see that p3 is characterized by a good voltage profile, the voltage set points are quite high, which is typical of the real losses minimization. To improve the other OFs, without getting to far from the p3 profile and with a maximum acceptable increase in losses of 5 MW, point p4 is obtained. Here the security is well improved, λ = 0.27, the reactive generation has increased of about 100 Mvar, while the losses only 2 MW. Finally, accepting a real losses increase inside the proposed margin, the CS is obtained in p5: the reactive generation is reduced by 600 Mvar (500 Mvar with respect to p3) and the security is maintained at the same level. The final voltage profile (Figure 9) is lower than p3 but better than p1 or p2. These results are very interesting: often the minimum losses criterion is not well accepted by the generation companies because it results in high voltage profiles; adopting the proposed multicriteria approach, the voltages result to be derived from the benefits given by each single OF.

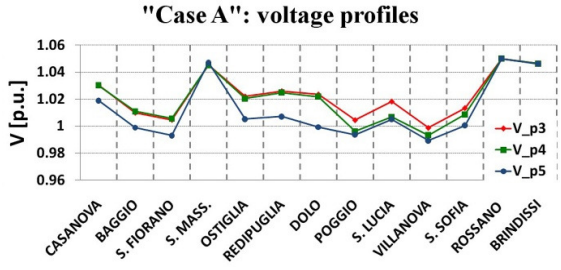

Figure 9: Voltage profiles: heuristic approach

For a better understanding of the voltage profiles behavior emphasized above, Figure 10 depicts the reactive levels for each control area and each DM point.

Figure 11 and Table 4 report the results of the DM for "Case B". Again, the first strategy gives two near points, p1 and p2, with a good security level and reduced reactive production, but with very high losses. Figure 12 reports the voltage profiles for these points. As it can be seen, they are more similar than in "Case A" due to the higher demand in the network.

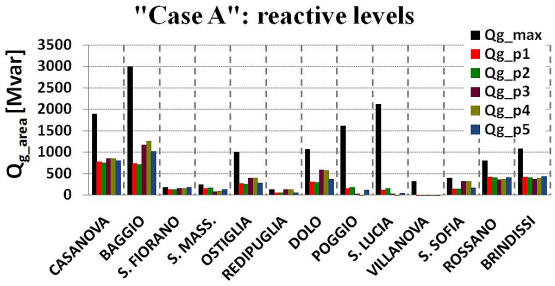

Figure 10: Reactive levels with different DM approaches

Applying the second heuristic DM approach, under the same requirements as "Case A", results in the p3-p4-p5 path of Figure 11. The voltage profiles are depicted in Figure 13. Again, the final voltage profile of p5 is better than the one of p1 or p2. Finally, Figure 14 shows the area reactive levels for each of the p1 – p5 points.

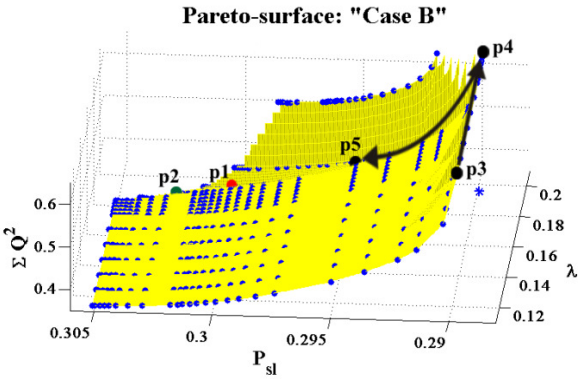

Figure 11: Decision making: "Case B"

	ΔP [MW]	$\sum\sum Q_k^r$ [Mvar]	λ	Load Margin [MW]
p1	393.7	5106	0.1965	6528
p2	395.6	4974	0.194	6445
p3	383.1	6236	0.1205	4003
p4	383.4	6238	0.199	6611
p5	387	5627	0.199	6611

Table 4: DM points: "Case B"

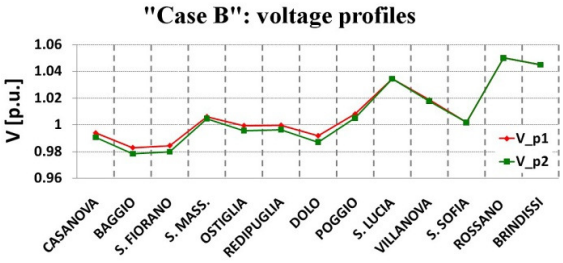

Figure 12: Voltage profiles: minimum distance DM criterion

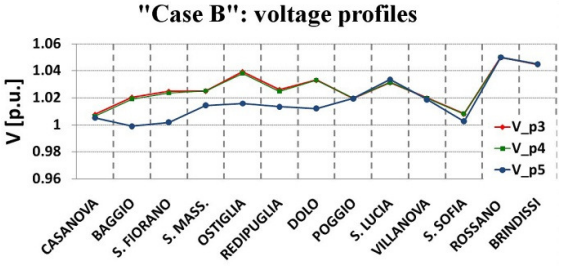

Figure 13: Voltage profiles: minimum distance DM criterion

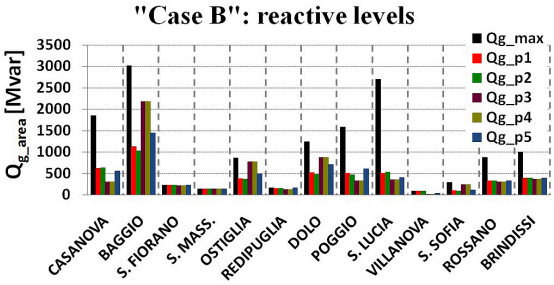

Figure 14: Reactive levels with different DM approaches

From the results reported in this paragraph we can conclude that choosing the CS according to the minimum distance criterion is not a good choice because: *i*) it is strongly dependent on the values of the OFs, which have a different meaning according to the nature of the goals and *ii*) it gives a good security level but it has the tendency to highlight the reactive generation objective function. The heuristic approach has the advantages of *i*) providing a more balanced point where the losses are also considered and *ii*) being more reasonable from the TSO perspective, used to adopt losses minimization. On the other hand, heuristic approach requires that the TSO adopts an active role in defining the criteria, i.e. the acceptable penalties, moving from p3 to p4 and p5. The definition of the Pareto-optimal solution curve results to be very useful.

5 CONCLUSIONS

The paper, based on a complete formulation of the HVC power flow equations, proposes an innovative multicriteria ORPF model. In particular, a novel complementary constraints formulation has been presented for the pilot nodes, investigating the differences with simpler models. Tests have been performed on a large size model of the Italian Transmission System, in order to correctly evaluate the robustness of the model with respect to a very non linear optimization problem.

Finally, a heuristic decision making procedure has been proposed to identify possible Compromise Solutions; for such a goal, the capability of the approach resulted to be very useful in identifying the most adequate procedure to be implemented by the decision makers for the identification of the optimal voltage profile.

DEDICATION

This paper is dedicated to the memory of our dear colleague and friend Prof. Paolo Marannino, an outstanding member of the Power Engineering community.

REFERENCES

[1] S. Corsi, M. Pozzi, C. Sabelli, A. Serrani, *The coordinated automatic voltage control of the Italian transmission grid*, IEEE Transactions on power systems, vol. 19, No. 4, November 2004.

[2] J. P. Paul, J.L. Lèost, J.M. Tesseron, *Survey of the secondary voltage control in france: present realization and investigations*, IEEE Transaction on Power systems, Vol. 2, No 2, Maggio 1987; pp. 505-511.

[3] P. Lagonotte, J.C. Sabonnaire, J.Y. Lèost, J.Y. Leost, J.P. Paul, *Structural analysis of the electrical system: application to secondary voltage control in France*, IEEE Transaction on Power Systems, Vol. 4, No 2, Maggio 1989, pp. 479-483.

[4] G. Franchi, M. Innorta, P. Marannino, C. Sabelli, "*Evaluation of economy and/or security oriented objective functions for reactive power scheduling in large scale systems*", IEEE Trans. on PAS, vol. 102, No.10, pp. 3481-3488, October 1983.

[5] A. Berizzi, C. Bovo, M. Delfanti, M. Merlo, C. Bruno, M. Pozzi, *ORPF Procedures for Voltage Security in a Market framework*, IEEE Power Tech 2005, S. Pietroburgo, Russia. 27-30 June 2005.

[6] J. L. Cohon, *Multiobjective programming and planning*, New York, Academic Press, 1978.

[7] V. Chankong, Y. Y. Haimes, *Multiobjective decision making: theory and methodology*, New York: North Holland series in science and engineering, vol. 8, 1983.

[8] A. Berizzi, C. Bovo, M. Innorta, P. Marannino, *Multiobjective optimization techniques applied to modern power systems*, IEEE PES Winter Meeting. Columbus (Ohio), USA. 28 January - 1 February 2001.

[9] T. R. Clemen, *Making hard decision – An introduction to decision analysis*, Belmont, California, USA: Duxbury Press, 1993.

[10] B. F. Hobbs, P. M. Meier, "*Multicriteria methods for planning: an experimental comparison*", IEEE Transaction on power systems, Vol. 9, No. 4, November 1994.

[11] A. Berizzi, C. Bovo, P. Marannino, *The Surrogate Worth Trade Off analysis for power system operation in electricity markets*, IEEE PES Summer Meeting, Vancouver, BC Canada, July 15-19, 2001.

[12] S. Corsi, P. Marannino, N. Losignore, G. Moreschini, G. Piccini, "*Coordination between the reactive power scheduling and the hierarchical voltage control of the EHV ENEL system*", IEEE Trans. on Power Systems, Vol. 10, No. 2, pp. 602-608, May 1995.

[13] A. Berizzi, C. Bovo, M. Delfanti, M. Merlo, D. Cirio, M. Pozzi, "*Online fuzzy voltage collapse risk quantification"*, Electric power system research, ISBN: 978-1-60692-613-0, 2008.

[14] W. Rosehart, C. Canizares, V. Quintana, *Costs of voltage security in electricity markets*, IEEE PES Summer Meeting, Vol. 1, Seattle, July 2000.

[15] W. Rosehart, C. Roman, A. Schellenberg, *Optimal Power Flow with complementary constraints*, IEEE Transactions on power systems, vol. 20, No. 2, May 2005

[16] R. Marconato, *Electric Power systems*, vol. 2, ISBN: 88-432-0025-9, CEI, 2004

[17] R. E. Rosenthal, GAMS – a users guide. [Online]. Available on: www.gams.com.